Photon- and Electron-Nucleon interactions in the 1st, 2nd and 3rd resonance regions - Part 1: summary of unsolved problems

George Smirnov

Photon- and Electron-Nucleon Interactions in the 1st, 2nd and 3d Resonance Regions Part 1: Summary of Unsolved Problems

G.I. Smirnov

Joint Institute for Nuclear research, 141980 Dubna, Russia

Laboratoire de Physique Corpusculaire de Clermont-Ferrand
IN2P3/CNRS – Univ. Blaise Pascal 63177 AUBIERE CEDEX FRANCE

Abstract

The Report contains an introduction to the physics of the lepton-nucleon scattering in the first three resonance regions, which correspond to the range of invariant masses W from 1.1 to ~ 2 GeV. It is emphasized, that large uncertainty in the determination of the limits of the validity of the perturbative QCD is related with poor understanding of the evolution of a resonance structure as a function of W and Q^2. The study of the VCS reaction and of its W dependence relatively to the π^0 electroproduction can have a number of advantages in pursuing the problem of the resonance structure evolution.

1 Introduction

Experimental and theoretical studies of the short-range nature of strong interactions between hadrons have a long history. Though many beautiful results were obtained, investigations did not advance at high speed as it was typical for some other fields of nuclear and particle physics.

On experimental side main difficulties were due to insufficient resolution of the spectrometers and limitations in luminocities in photon and electron beams experiments. Pion-nucleon scattering experiments offered high statistics data but, as it turned out, could not produce evidence for existing of a number of resonance states around $W = 2$ GeV predicted by quark models [1]. There are reasons to speculate that the predicted states may not couple significantly to the πN channel. They may decay predominantly into $\pi\Delta$, ρN, or γN. In such cases new generation experiments on photo- and electroproduction could be decisive for discoveries of the missing resonance states.

On theoretical side there was always a very serious obstacle, namely a large value of the strong coupling constant, which did not allow to apply the well developed methods of perturbation theory. This is why the theory which is to be developed for the resonance region is being called non-perturbative QCD.

Perturbative QCD Lagrangian describes interaction between pointlike quarks and gluons. There exists an essential difference between coupling of the field with a pointlike elementary particle and with a hadron, which has a composite internal structure. In the first case the coupling is determined by dimensionless parameters, for example the charge of the particle and its magnetic moment. In the second case the coupling depends on the size of the interaction region, and, as a result, on the momentum transferred to the particle. This is where form factors [2] (exclusive reactions) and structure functions [3] (inclusive reactions) appear. The finite size of the nucleon reveals itself also in the Compton scattering off protons (the reaction with zero momentum transfer) as the electric and magnetic polarizabilities of the proton [4, 5].

Some theorists believe that perturbative QCD can be applied for consideration of the exclusive reactions in the resonance region (c.f. ref. [6]). No consistent quantitative description of the data in the PQCD framework is available so far. It is reasonable to assume that the transition from the region of hadronic physics to the QCD regime at some given Q^2 can occur in one specific channel only. A rise of experimental activity at MAMI and CEBAF, which we witness these days, allows one to confront numerous PQCD predictions with high precision data.

Numerous models of hadrons have been suggested for the description of the data collected in experiments on photo- and electro-production of pions (c.f. review [7, 8]). They are:
 – isobaric models [7, 9],
 – dispersion models [10, 11],
 – nonrelativistic and relativistic quark models [12–16],
 – effective Lagrangian approaches [17],
 – quark bag models [18, 19],
 – Skyrm models [20, 21, 22],
 – soliton models [23].

As a rule, models start with different assumptions and introduce a number of parameters which are to be found from experiments. As a result, many quantities obtained from experiments with the help of the models, like the ratio of electric quadrupole to the magnetic

dipole amplitudes $E2/M1$, become model-dependent.

On the other hand, a good description of the data in a model independent way is offered by phenomenological approaches (c.f. [24]) that serve many practical purposes. Phenomenological approaches which were developed for the analysis of the data on pion photoproduction [25] proved to be very effective for the understanding of the physics of hadronic interactions in the absence of a theory. In this way one obtains a quantitative information on the amplitudes of the pion photoproduction, which is then used in the studies of (1) isotopic structure of the electromagnetic current of the hadrons, (2) parity conservation in electromagnetic interactions of hadrons, (3) πNN^* transition form factors etc.

2   Hadronic Form Factors

Hadronic form factors describe the distribution of charge and current inside a hadron as a function of the momentum Q^2 transferred from the virtual photon, which serves as a probe of the structure. It is not evident if the concept of the static spatial distributions of charge and current is still valid at distances less than the proton's Compton wavelength. This is why one uses two different decompositions of the current into parts, which contain form factors. In the first one, the current is decomposed into $F_1(Q^2)$ and $F_2(Q^2)$ parts, which are the Dirac and Pauli form factors, respectively. In the second approach the scattering amplitude is decomposed into a non-spin-flip part and a spin-flip part which are related with the Sachs form factors $G_E(Q^2)$ and $G_M(Q^2)$, respectively. The relation between F_1 and F_2 and the Sachs form factors is

$$G_E(Q^2) = F_1(Q^2) - \tau \kappa F_2(Q^2),$$
$$G_M(Q^2) = F_1(Q^2) + \kappa F_2(Q^2),$$

where $\kappa = 1.793$ is the anamolous magnetic moment of the proton and $\tau = Q^2/4M^2$. By the definition, at $Q^2 = 0$, $G_E = 1$ and $G_M = 1 + \kappa = 2.793$.

It has been found in the classical experiments on elastic electron-proton scattering that the proton electric form factor has a dipole behaviour

$$G_E^p(Q^2) \approx G_D(Q^2) \equiv \frac{1}{(1 + Q^2/\Lambda^2)^2} \ ,$$

where $\Lambda^2 \approx 0.71$ GeV^2 [2].

Most recent experiments (c.f. ref. [26]) observe that G_E^p falls more rapidly with Q^2 than the dipole form factor G_D. Even more important is the observation [26] that G_E^p falls faster than G_M^p in contrast with many models of the proton structure. On the other hand, if one considers the proton as a conductor, it is rather natural to expect the different spatial distributions of the charge and magnetization currents in the proton. Precise determination of G_E^p and G_M^p is of fundamental importance for the understanding how the proton structure evolves in the nucleon exited states.

The form factor concept is also useful for parametrization of the Q^2 dependence of the total cross sections for pion electroproduction in the resonance region [27]. Such form factors are often called $\gamma N\Delta$ (or γNN^*) transition form factors to underline their role in determining the $N\Delta$ (or NN^*) transition amplitude into a given resonance state. They are introduced with the requirement to respect the analytic structure of the amplitude, which is (in the

simplest way) a product of poles lying on the real Q^2 axis. The number of poles required in a given form factor is determined by the angular momentum of the state.

3   Nucleon Resonances. Basic notations

In the present Report I make use of an opportunity to comment on feasibilities of the JLAB experiment E93050 [28] to inverstigate the structure of resonances. The data collected by E93050 belong to the range of invariant masses W from 1.1 to $\sim$ 2.0 GeV. This is where the three resonance regions, the first – $W \sim 1232$ GeV, second – $W \sim 1535$ GeV, and third – $W \sim 1700$ GeV, have been identified in the early experiments on pion-nucleon scattering and in the pion photo- and electroproduction experiments [29, 30]. Clear resonance structure in the total photoabsorption cross section for the proton is displayed in Fig. 1 borrowed from ref. [8].
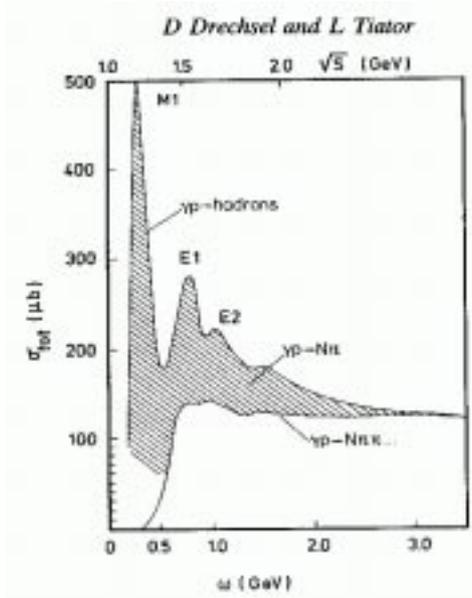

Fig. 1. The total photoabsorption cross section for the proton and its decomposition into exclusive channels as a function of the photon energy ω (l.s.)

The intermediate πN state is classified according to the quantum numbers as follows: [1] $L_{2I \cdot 2J}$, where $L =$ S, P, D, F, ... if the orbital angular momentum $l = 0, 1, 2, 3, ...$ respectively, $I = \frac{1}{2}$, $\frac{3}{2}$ is the total isospin (or intermediate state isospin), $J = |l \pm \frac{1}{2}|$ is the total spin (or intermediate state spin). An example of the classification can be found in Table 1. The angular momentum is related to the spin J and parity P of the resonance state: $l = J - 1/2$ if $P = +1$ and $l = J + 1/2$ if $P = -1$. The same resonance state can be excited at different values of W, so in addition one has to use the resonance name, which is either N (if $I = \frac{1}{2}$) or Δ (if $I = \frac{3}{2}$) followed with its mass, e.g. $\Delta(1232)$ for P_{33} state.

---

[1]the definition is now used by the Particle Data Group

State	l	J	Helicity element
S$_{11}$	0	1/2	A_{0+}
S$_{31}$	0	1/2	A_{0+}
P$_{11}$	1	1/2	A_{1-}
P$_{31}$	1	1/2	A_{1-}
P$_{33}$	1	3/2	A_{1+}
			B_{1+}
D$_{13}$	2	3/2	A_{2-}
			B_{2-}
D$_{15}$	2	5/2	A_{2+}
			B_{2+}
F$_{15}$	3	5/2	A_{3-}
			B_{3-}
F$_{35}$	3	5/2	A_{3-}
			B_{3-}
F$_{37}$	3	7/2	A_{3+}
			B_{3+}

Table 1. The resonance states observed in pion photoproduction in the range $W < 2$ GeV [30]. The definition of the states, as they are reviewed by Particle Data Group, is as follows:

The state: $L_{2I \cdot 2J}$,

where $L =$ S, P, D, F, ...   if the orbital angular momentum $l = 0, 1, 2, 3, ...$ respectively,
$I = \frac{1}{2}, \frac{3}{2}$ is the total isospin,
$J = |l \pm \frac{1}{2}|$ is the total spin.
Helicity elements $A_{l\pm}$ and $B_{l\pm}$ correspond to excitation of resonances by transversely polarized photons which result in the initial states of $\lambda = 1/2$ and $\lambda = 3/2$ respectively.

3.1   Isospin structure of matrix elements

The matrix element of the photoproduction reaction evaluated under the assumption of isospin conservation contains three components which are related with the isovector electromagnetic current – $A^{(-)}$ and $A^{(+)}$, and with the isoscalar current – $A^{(0)}$:

$$A = A^{(+)}\delta_{\alpha 0} + \frac{1}{2}A^{(-)}(\tau_\alpha \tau_0 - \tau_0 \tau_\alpha) + A^{(0)}\tau_\alpha,$$

where τ are the Pauli matrices, and α is the pion isospin index. The introduced isospin amplitudes can be used for the evaluation both of the amplitudes of the four photoproduction reactions – $A(\gamma N \rightarrow N\pi)$,

$$
\begin{aligned}
A(\gamma p \rightarrow n\pi^+) &= \sqrt{2}(A^{(-)} + A^{(0)}), \\
A(\gamma p \rightarrow p\pi^0) &= A^{(+)} + A^{(0)}, \\
A(\gamma n \rightarrow n\pi^-) &= -\sqrt{2}(A^{(-)} - A^{(0)}), \\
A(\gamma n \rightarrow n\pi^0) &= A^{(+)} - A^{(0)}.
\end{aligned}
$$

and of the amplitudes of the transition into a specific state defined by the isospin I of the πN system – $A^{(I)}$,

$$A^{3/2} = A^{(+)} - A^{(-)} \quad (I = \frac{3}{2}),$$

$$A^{1/2} = A^{(+)} + 2A^{(-)} \quad (I = \frac{1}{2}),$$

$$A^0 \quad (I = \frac{1}{2}).$$

3.2 Transition current structure

The structure of the transition current between initial and final nucleon states is obtained from most general requirements of the Lorenz, gauge and P-invariance. It can be shown, that the number of independent spin operators for the amplitude of the binary process involving photons is given by

$$n = 2(\sigma + 1)(2\sigma + 1),$$

where σ is the particle spin. For the photon-nucleon reaction $n = 6$, which defines therefore the number of independent amplitudes F_i, $i = 1 \div 6$ (c.f. ref. [8]). The amplitudes F_1, F_2, F_3 and F_4 describe the transverse current, and the longitudinal component is given by F_5 and F_6. They depend on three variables, — 4-momentum transfer Q^2 and on two Mandelstam variables s and t. The two latter can be of course replaced with the photon energy $\omega_{\text{l.s.}}$ and the pion c.m.s. angle θ^*. The amplitudes are complex which is the consequence of the strong interaction in the πN system. The way they are introduced relate them with spin degrees of freedom of interacting particles which means, that their complete determination is not possible without polarization experiments.

3.3 Helicity amplitudes

Phenomenology of the photo- and electroproduction reactions allows one to bypass unsolved theoretical problems of evaluation of F_i - amplitudes. The observables can be expressed in term of six parity conserving helicity amplitudes H_i, which are defined by transitions between eigenstates of the helicities of nucleon and photon. Helicity amplitudes have a complicated kinematic structure but in spite of that are widely used because of their elegant angular momentum properties and their general applicability to arbitrary spin.

Further simplification is achieved by the angular momentum decomposition of H_i, which can be expanded in terms of derivatives of Legandre polynomials (c.f. ref. [7]). This yields the partial wave (PW) helicity elements $A_{l\pm}$, $B_{l\pm}$ and $C_{l\pm}$ which depend on W and Q^2.

$A_{l\pm}$ and $B_{l\pm}$ are the transverse PW helicity elements for $\lambda_{\gamma N} = 1/2$ and $\lambda_{\gamma N} = 3/2$, respectively. $C_{l\pm}$ are the longitudinal PW helicity elements. One can relate the PW helicity elements to the magnetic, electric, and scalar (longitudinal) multipoles $M_{l\pm}$, $E_{l\pm}$ and $S_{l\pm}$. A transition is defined to be **magnetic** with multipoles $\boldsymbol{M_{l\pm}}$ if the total angular momentum absorbed from the photon is $\boldsymbol{l}$ and **electric** with multipoles $\boldsymbol{E_{l\pm}}$ if the total angular momentum absorbed from the photon is $\boldsymbol{l \pm 1}$. The corresponding **scalar** (longitudinal) multipole is $\boldsymbol{S_{l\pm}}$. If $J = l + 1/2$ the process can be described in terms of the multipole amplitudes M_{l+}, E_{l+} and S_{l+} as (c.f. ref. [34])

$$
\begin{aligned}
M_{l+} &= \frac{1}{2(l+1)}[2A_{l+} - (l+2)B_{l+}], \\
E_{l+} &= \frac{1}{2(l+1)}[2A_{l+} + lB_{l+}], \\
S_{l+} &= \frac{1}{l+1}\frac{|\vec{k}^*|}{Q}C_{l+},
\end{aligned}
\tag{1}
$$

where $\vec{k}^*$ is the photon three-momentum in the hadronic rest frame. If $J = l - 1/2$ the process is described by M_{l-}, E_{l-} and S_{l-} with

$$M_{l-} = \frac{1}{2l}[2A_{l-} + (l-1)B_{l-}],$$

$$E_{l-} = \frac{1}{2l}[-2A_{l-} + (l+1)B_{l-}], \tag{2}$$

$$S_{l-} = -\frac{1}{l}\frac{|\vec{k}^*|}{Q}C_{l-}.$$

Helicity amplitudes are therefore expressed as:

$$A_{l+} = \frac{1}{2}[lM_{l+} + (l+2)E_{l+}],$$

$$B_{l+} = -M_{l+} + E_{l+}, \tag{3}$$

and

$$A_{l-} = \frac{1}{2}[(l+1)M_{l-} - (l-1)E_{l-}],$$

$$B_{l-} = M_{l-} + E_{l-}. \tag{4}$$

Angular distribution of the outgoing pions essentially depends on the type of the transition. Some examples of modifications of the $d\sigma(\theta^*)/d\Omega$ are shown below and are displayed in Figure 2:

Magnetic dipole —	M_{1+}	:	$2 + 3\sin^2\theta^*$
Electric quadrupole —	E_{1+}	:	$1 + \cos^2\theta^*$
Magnetic quadrupole —	M_{2-}	:	$1 + \cos^2\theta^*$
Electric octupole —	E_{2-}	:	$5 + 6\cos^2\theta^* + 5\cos^4\theta^*$

The PDG [29] presents results of the measurements of the resonance states obtained after subtraction of nonresonant background. The total photoabsorption cross section for the transition into a specific resonance is then written as follows:

$$\sigma_{tot} = \frac{2M}{W_r\Gamma}(A_{1/2}^2 + A_{3/2}^2). \tag{5}$$

The amplitudes $A_{1/2}$ and $A_{3/2}$ are related with $\tilde{A}_{l\pm}$ and $\tilde{B}_{l\pm}$ which are free from the background with the help of isospin coefficients.

4 Non-Resonance Continuum

Non-resonance part of the measured cross sections is generally related with the contribution from the s channel amplitude of the reaction in question. It can not be negligible because of closeness to the nucleon pole $s = M^2$. The contribution from the two other channels, t and u, is considerably smaller and is strongly model dependent [9]. This is sometime called as a "structure of the Born terms", which is fairly well known for the pion electro-production in the first resonance region, somewhat worse for higher resonances, and unknown for η electro-production in the second resonance region [31]. Non-resonance contribution to the cross sections of the baryon resonance production is often called as "background contribution". Its subtraction from the data is not trivial because of the interference of the resonance amplitudes with the background ones. The interference can be considered as the
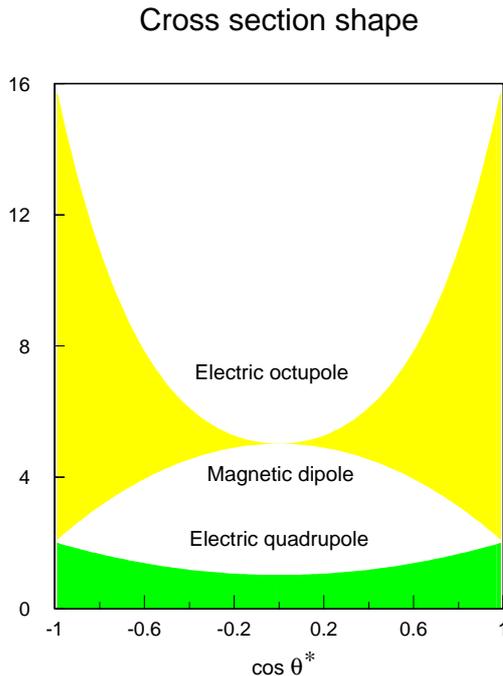
Cross section shape

Figure 2: Variation of the differential cross section of the resonance pion photoproduction as a function of the pion angle θ^* for three different transition amplitudes

modification of the bare resonance vertex. To put the other way round, the measured cross section corresponds to the "dressed" resonance vertex.

In the first resonance region the Born terms contribution can be evaluated in the dispersion relation approach without free parameters if unitarity and pion-nucleon phase shifts are used. As long as the background contribution here is small the calculations can be realized by iterations. This is not applicable in the higher W regions where the contribution from the Born terms increases and eventually becomes larger than that from resonances. Thus, Figure 3 displays almost linear rise of the non resonance contribution as a function of W evaluated in the framework of the isobar model [9] at fixed π^0 emission angle $\theta^* = 180^0$ and $Q^2 = 1$ GeV^2. Such behaviour is understood as evolution of the final state interaction (FSI) and has been taken into account in ref. [9] by means of the unitarization of the pion electroproduction amplitude. The study of the angular dependence which I have performed with program MAID [9] for three values of W is shown if Figure 4. The rise of the Born terms contribution is particularly spectacular at the backward direction ($\theta^* = 180^0$) when W reaches the region of the second and the third resonance.

A model independent evaluation of the non resonant part of the cross section can hardly be feasible in the Q^2 range of the E93050 experiment because of the essentially non-local character of interaction between the particles in the final state. Indeed, one have to bear in mind that the radius of the interaction region is ~2 fm, and the radii of the pion and the nucleon are ~0.6 and 0.82 fm, respectively. The interaction is of a relativistic nature, and one has do deal with the off-mass shell nucleon in the intermediate state. Relativistic treatment of the process requires consideration of a large number of diagrams (which means that in the same interaction volume one finds a lot more objects) including terms with N$\overline{\text{N}}$
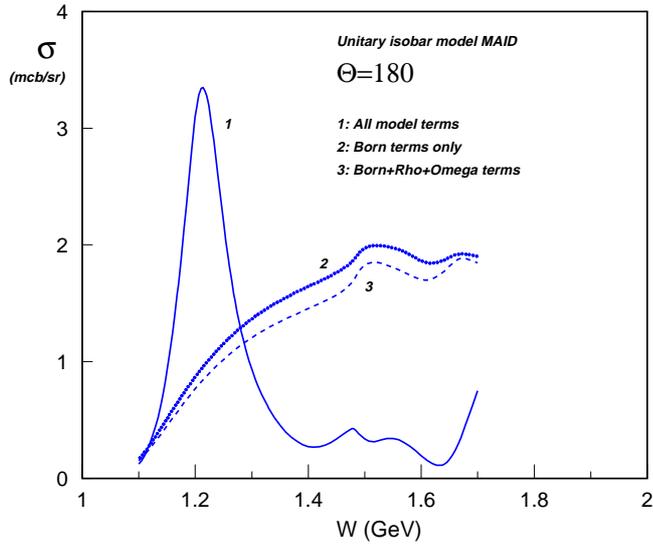
8

Figure 3: Differential cross sections of the π^0 electroproduction as a function of W evaluated in the region of three resonances using program MAID of ref. [9]. Contribution of all terms is displayed with the full line (1), contribution of the Born terms only is shown with the dotted line (2) and contribution of all nonresonant terms is shown with the dashed line (3)

pairs. In the higher Q^2 region many diagrams which contribute to the final state interaction (FSI) are suppressed as $1/(Q^2)^l$, $l \geq 2$, and theoretical consideration becomes realistic. Still, the technique is only being developed (see review [33]). Suppression of the Born terms contribution in the higher Q^2 region as it can be evaluated in the isobar model is illustrated in Figure 5.
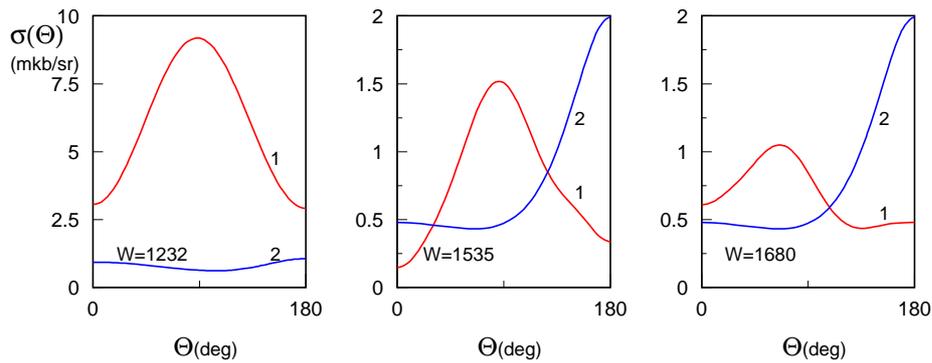

Figure 4: Differential cross sections of the π^0 electroproduction as a function of the pion angle θ^*. Full lines display contribution of all terms – 1, and of Born terms only – 2

9

The investigation of the virtual Compton scattering (VCS) reaction

$$e^- + p \rightarrow e^- + p' + \gamma$$

can be considered as very promising for the understanding of the FSI problem because its products do not interact strongly. Particularly interesting will be results on W dependence of the VCS cross sections in the second and third resonance regions, where unitarization procedure is strongly model dependent. The results from VCS studies will be also helpful in understanding of the whole class of hadronic reactions with the pion and nucleon in the final state.
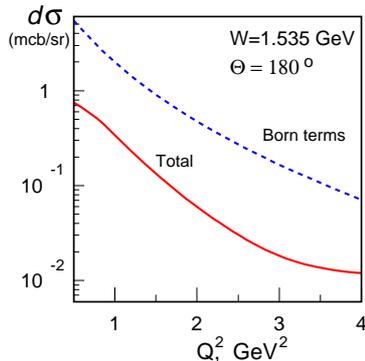

Figure 5. The differential cross section for the π^0 electroproduction evaluated in the Unitary Isobar Model [9] (program MAID) at fixed $W = 1.535$ GeV and $\Theta^* = 180^0$

5 The Nucleon Compton Scattering in the $\Delta(1232)$ Region

5.1 Real Compton scattering

Phenomenological approaches which offer parameter free predictions for future experiments are most welcome for consideration of the photo- and electroproduction reactions it the resonance region. In ref. [24] it is suggested to connect in a model-independent way the cross sections for pion photoproduction reactions and the Compton amplitudes for the excitation of the $\Delta(1232)$. The analysis of [24] has been inspired by a high precision determination of multipole amplitudes for the pion photoproduction reactions by Grushin *et al.* [25]. The work is unique because the real and imaginary parts of the multipole amplitudes have been determined *independently*, which never was done previously. To understand how it is important one has to recall that the photoproduction amplitudes are related with the exact unitarity theorem (Fermi-Watson, or simply Watson theorem). Of course, since the cross section of the Compton scattering (CS) reaction is two orders of magnitude smaller than that of pion production, one can stay with approximate form of the unitarity theorem by fixing the phase between real and imaginary parts of a given multipole amplitude with just strong pion-nucleon phase shift $\delta^{\pi N}$. Alternatively, the analysis of Grushin allows one to determine the sum of the Compton and pion nucleon phase shifts — $\delta^{CS} + \delta^{\pi N}$. This can eventually be used in the consideration of the 2×2 **S** matrix, which corresponds to two fundamental principles — unitarity (that is, $\mathbf{S}^+\mathbf{S} = 1$) and time-reversal invariance.

The unitarization procedure developed in ref. [24] allows one to estimate Compton scattering cross section in the region of $\Delta(1232)$ resonance with the help of existing data on the
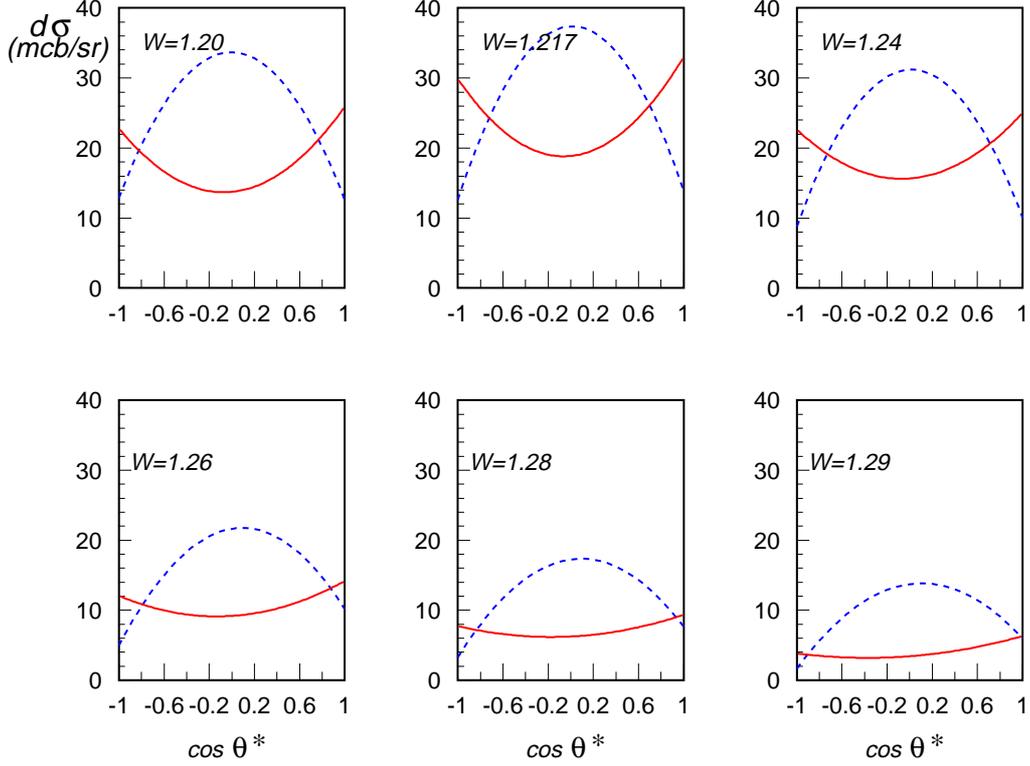
Figure 6: Differential cross sections of the π^0 photoproduction (dashed curves) and of the Compton scattering (solid curves) as a function of the c.m.s. angle θ^* evaluated in the region of $\Delta(1232)$ resonance. Results for Compton cross sections are scaled by factor 100, values of W are in GeV

pion photoproduction. The procedure is however an approximation, because it allows one to compute imaginary parts of the transition amplitudes but not the real ones. In this way one obtains the unitary *lower bounds* of the differential cross sections $d\sigma/d\Omega$. The results for the two processes are displayed in Figure 6 as a function of $cos\theta^*$ for six values of W where the analysis of pion photoproduction [25] has been performed.

If one assumes that the magnetic dipole transition amplitude dominates, the expression for the cross section simplifies very much:

$$\frac{d\sigma}{d\Omega} \simeq \frac{3cos^2\theta^* + 7}{2}|f_{MM}^{1+}|^2, \tag{6}$$

where f_{MM}^{1+} is the helicity amplitude which represents the transition $M1 - M1$. Imaginary part of f_{MM}^{1+} determined in ref. [24] is for example $(16.813 \pm 0.766)10^{-4}/m_\pi$ at the photon energy $E_\gamma = 320$ GeV. This fully symmetric cross section is displayed in Figure 7 along with the Compton scattering cross section obtain with the set of multipoles of ref. [24]. The difference between the two curves could serve as a measure of comtribution of the electric transition amplitude to the Compton scattering cross section. It is displayed in the right panel of Figure 7 as the ratio of two cross sections considered in the limited range of the c.m.s. angle θ^*, which corresponds to the kinematics of the E93050 experiment.
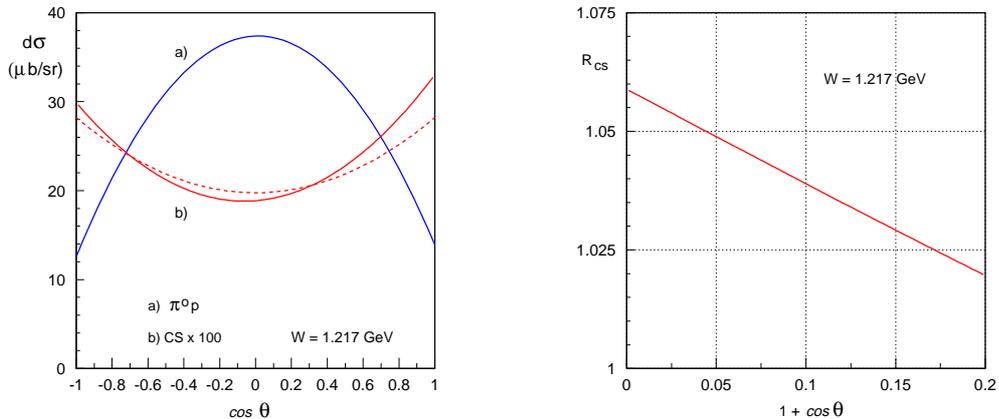
11

Figure 7: Left panel: Differential cross sections of the π^0 photoproduction (full line a)) and of the Compton scattering (full line b)) as a function of the c.m.s. angle θ^* evaluated at W = 1.217 GeV. Results for Compton cross sections are scaled by factor 100 and are shown with a full line when magnetic and electric transition amplitudes are used for calculations, and with a dashed line for the magnetic dipole transition amplitude. Right panel: Effect of non-zero contribution from the electric transition amplitudes shown in a limited interval of θ^* as the ratio of the Compton cross sections displayed in the left panel

5.2 Virtual Compton scattering

The measurement of the ratio $R(W)$ of the cross sections for the backward production of π^0 and photons is a part of the E93050 experimental program. The ratio can be accessed in a wide range of W and at $Q^2 \sim 1$ GeV^2. I use the results displayed if Figure 6 to estimate $R(W)$ in the backward direction – $\theta^* = 180^0$. The obtained ratio – $R \sim 2.5\%$ – is shown in Figure 8. It corresponds to $Q^2 = 0$ and only slightly varies with W in a drastic contrast to resonance behaviour of the cross sections. It is not expected to vary significantly as a function of Q^2 in the range of Q^2 from 0 to ~ 1 GeV^2. The physics which is behind the W and Q^2 independence of R is of particular interest because it is related with both the resonance size and structure and the strong interaction radius r_s. As long as the structure of $\Delta(1232)$ is defined by the dominant magnetic dipole transition M_{1+}, it is frozen within the considered range of W. Also the same for the two reactions are the mean-square radius of the resonance $\langle r_\Delta^2 \rangle$ and r_s. This determines the W independence of R.

Higher partial waves are switched on with the increase of W, which have to change noticeably angular dependence in both channels. This can result in changes of R because of different restructuring effects in the π^0 and VCS channels. The restructuring process has a unique topological restriction determined by the same (or almost the same) size of r_s and a resonance $\langle r_{\Delta(N)}^2 \rangle$. If we assume that all resonances are of the same size than the variations in R versus W are determined by evolution of two factors: (1) the resonance structure and (2) strong FSI in the nonresonant production of π^0. $R(W)$ measured at $\theta^* = 180^o$ is expected to decrease in a *smooth* way if nonresonant contribution dominates or in a *step-like* way if the effects of resonance restructuring are more important that FSI effects.

It would be interesting to measure $R(W)$ independently for N^* and Δ resonances because
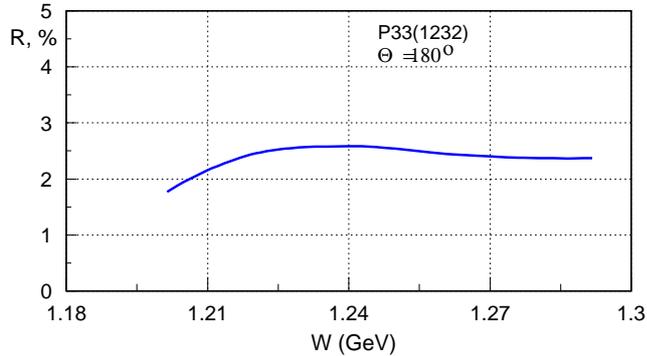
Figure 8: The ratio of cross sections of Compton scattering to π^0 photoproduction as a function of W

its evolution is related with the resonance spin rather than with W. The difference between structure of N^* and Δ is indeed of fundamental origin and follows from the Regge theory. More specifically, one Regge pole contributes to all partial waves which belong to the same trajectory. Because of the finite value of r_s and finite number of different structural states (one deals with the quantum process) one anticipates that R will saturate somewhere at the boundary between baryon resonances and PQCD region. In the region of saturation R is expected to be determined by the ratio of the mean-square radii of the strong interaction and proton, which is ~ 9. Therefore, the variation of $R(W)$ between its minimal and maximal values could serve as a model independent measure of the strong interaction radius r_s.

6 Relation with the PQCD Predictions

As long as QCD is a theoretical consideration only of the evolution of the structure of hadrons it can not determine the moment when the perturbative regime sets on. It is up to an experiment to find the conditions in which data agree with the PQCD predictions. One of such predictions concerns the Q^2 behaviour of the helicity amplitudes A_{1+}, B_{1+} and C_{1+} measured in the pion electro-production reaction in the region of $\Delta(1232)$ (or P$_{33}$ resonance state in Table 1). The first one – A_{1+} – is helicity-conserving ($\Delta\lambda = 0$), while two other are helicity-non-conserving ($\Delta\lambda = 2$ and $\Delta\lambda = 1$ for B_{1+} and C_{1+} respectively). At high Q^2 (which is to be determined) PQCD predicts that the helicity-conserving amplitude A_{1+} dominates and B_{1+} and C_{1+} asymptotically approach zero [6]. If expressed as $A_{1/2}$ and $A_{3/2}$ amplitudes, this corresponds to $A_{1/2} \gg A_{3/2}$.

According to Eq. (3) the helicity amplitudes for the P$_{33}$ state can be written as follows:

$$
\begin{aligned}
A_{1+} &= (1/2)M_{1+} + (3/2)E_{1+}, \\
B_{1+} &= -M_{1+} + E_{1+}, \\
C_{1+} &= (Q/\vec{k}^*)S_{1+}.
\end{aligned}
\tag{7}
$$

As it follows from Eq. (7), in the QCD regime $E_{1+} = M_{1+}$, or, equivalently, the ratio

13

$R_{EM} \equiv E_{1+}/M_{1+} = 1$. At the moment, the experimental data on R_{EM} are available in the range of Q^2 up to 4 GeV^2 . The ratio is found to be small independently of Q^2 and negative when evaluated in the framework of the effective Lagrangian model [32], but positive if it is extracted within the dispersion relation approach [10]. The experimental value is also in a good agreement with the earlier analysis of ref. [17].

The suppression of the $A_{1/2}$ amplitude, which is being favored by the present data, is understood as a cancellation in the leading-order term of the matrix elements connecting the symmetric $\Delta(1232)$ distribution amplitude with the symmetric and antisymmetric proton distribution amplitude [6]. This might result in the dominance of the $A_{3/2}$ amplitude in a fairly wide range of Q^2 which needs experimental verification.

7   What is missing: the resonances or understanding?

The hunt for the new resonance states has been always supported by convincedness that it is just a matter of experimental technique to register a state allowed by symmetry considerations. This comment applies everywhere, not only when one deals with Δ or N* states. The symmetries beyond doubt are the stronghold of theoretical predictions as long as the effects of the internal structure are negligible. A fundamental SU(2) symmetry serves as a good example: small difference in the internal structure of the proton and neutron does not result in different properties of their nuclear interactions. It is not that simple with the resonances which undergo restructuring each time their spin J is increased. With evolution of the internal structure the nice symmetry picture turns into a mess: resonance peaks overlap, they mix and interfere. In theoretical language it means that the decay amplitudes become "structure-dependent" [35]. As a result, predictions of the models become unreliable. Indeed, in some cases, parametrization of baryon structure considered in ref. [35] would require 28 mixing angles while the available data correspond only to few measured decay amplitudes.

To my understanding, many theoretical difficulties could be resolved if one considered the differences in structure of resonance states as a manifestation of the same fundamental property of strong interaction, namely invariance of the interaction range limited by $r_s \sim 2$ fm. It is reasonable to assume that all resonances are of the same size, because the simplest way to form an excited state is to occupy the entire space volume allowed by the interaction range. This condition will define not only evolution of the spin states but also relative decrease of the resonance amplitude with increasing J.

In this picture the resonance structure is defined by

- electromagnetic current conservation — div $\mathbf{j} = 0$,

- requirement of the twofold symmetry between the current circuits which get split due to excitation — $\mathbf{j}_n = \mathbf{j}/2^{n-1}$,

- requirement of either the finite length (or size) of the smallest current circuit or the smallest current density (the highest excited baryon state).

The three requirements are of fundamental nature and are therefore model independent. If they are fulfilled, the electric and magnetic properties of a resonance evolve with increase of W in full accordance with the observed dipole, quadrupole, etc. excitations. In addition, one obtains the structure which always depends on the structure (and therefore on the

amplitude) of the previouse resonance state. Such an evolution ends up in the transition to the PQCD region where the electromagnetic current is defined by the structureless partons.

Non-perturbative character of the evolution follows from the second requirement: each transition results in complete restructuring of the resonance and not in small (compared to initial state) perturbation.

The picture of evolution considered here is supported by a number of experimental evidence. The best one is the Bloom-Gilman duality, which is a demonstration of close relation between W and Q^2 behaviour of the electroproduction of nucleon resonances and the Q^2 behaviour of the deep inelastic electron-nucleon scattering when $Q^2 \geq 1$ GeV^2 [36]. Such a relation would not have existed if the structure of the resonance states evolved with W independently of the previouse states. To put it in another way, all resonances are aware of (1) their ancestors, (2) their inheritors, and (3) the nonresonance background. They also exactly know that at a certain point (line ?) at the $W-Q^2$ surface their unexplicable internal structure will be replaced by the elegant partonic structure of the nucleon.

The transition of the baryon matter into the PQCD regime, which is described by Bloom and Gilman as "appropriate averaging of many broad resonances and background" is actually the process of the nucleon topology modification. One can as well treat it as a degradation of the electrical conductivity of the nucleon which results from the splitting it into separated conductive regions. This phenomenon is never considered in the models of the hadronic structure.

Naturally, results of evolution of the resonance structure depend on the structure of the initial state. This is where one can not neglect even small differences between the states with different isospin. Indeed, as it is known from the Regge model, Δ- and N*-resonances belong to different Regge trajectories. Furthermore, the lowest state on the Δ trajectory is P$_{33}$, while it is S$_{11}$ on the N* trajectory. The concept of Bloom-Gilman duality has been formulated for the N* resonances. There are many reasons to believe that it is applicable to Δ's as well but with different Q^2 dependence near $\Delta(1232)$. Indeed, the duality picture assumes at least two necessary conditions for the transition to the partonic regime: (1) $Q^2 \to \infty$ and (2) W (or J) $\to \infty$. If considered qualitatively, both conditions could be satisfied with the simplest relation which I assume as $Q(J - J_0) = \mathbf{C}$, where J_0 is the Regge trajectory intercept. For illustration I have chosen three values of arbitrary parameter $\mathbf{C}$ such that the QCD regime is switched on at $Q^2 = 4$, 10 and 20 GeV^2 at $J = 0$ when one stays with the N* trajectory. This particular choice of $\mathbf{C}$ serves to discribe widely discussed uncertainty in the position of the boundary, which is in the present examples lies (see Figure 9) somewhere between 1 and 5 GeV^2 for higher resonance states.

The difference in the intercept for the two trajectories results in very different behaviour of the boundary in the low J region. This implies that transition to the QCD regime might be reached earlier in the studies of N* resonances. It is also clear that the study of W dependence in the experimental conditions of the E93050 experiment can have a certain advantage in the search of the PQCD regime compared to the study of the Q^2 dependence.

8   Backward electroproduction of π^0 and VCS

The evolution of structure of Δ and N* states has to be considered as related to the modification of the exchange forces within the restricted volume defined by the radius of strong interaction r_s. This is why I expect that the ratio of VCS to π^0 electroproduction cross
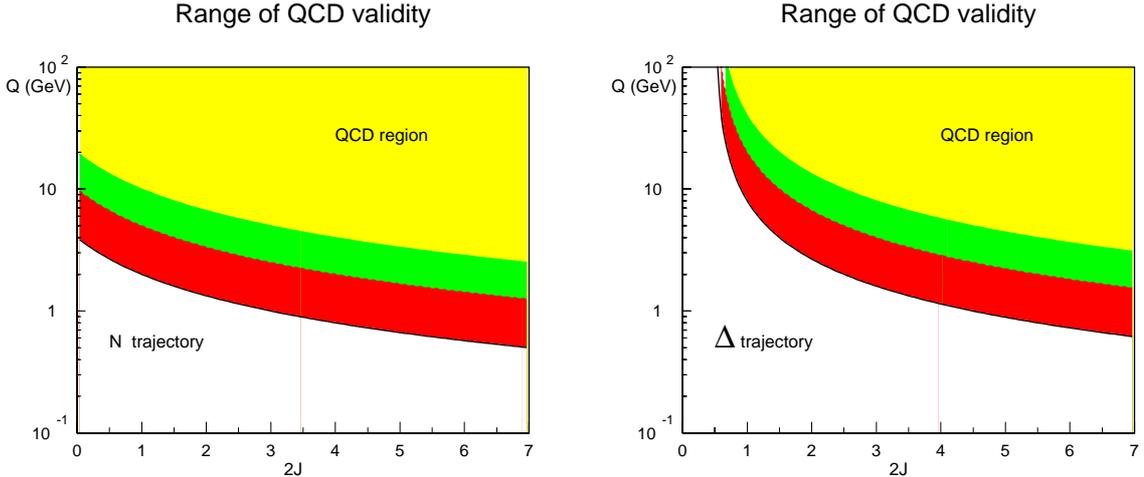
Figure 9: The boundary between baryon resonances region and the PQCD region estimated for different $\mathbf{C}$ defined as $Q(J - J_0) = \mathbf{C}$

sections will evolve with W when measured at a certain fixed angle θ^*. The advantage of using the backward electroproduction for the data taking is evident from nature of the structure modification. Indeed, for the lowest state $– l = 0$, the angular distribution of pion is isotropic. The subsequent modifications (l increases) of the structure change the shape of the angular distribution in such a way that the outgoing pions are directed predominately at the angles $\theta^* = 0$ and 180^0. So far the consideration does not involve any model assumption. The evolution of Born terms contribution, which to my understanding should not be considered as background, will modify the symmetric pattern the angular distribution. They (Born terms) can hardly increase the albedo of incident photons (see discussion in ref. [37]) but can increase manyfold the signal from π^0.

Conclusion

The revived interest in the investigation of the physics of resonances is not just a search of missing resonances with modern accelerator facilities. It is rather the search of understanding of the evolution of the baryon matter structure in extremely difficult for experimental observation conditions. Actually, the same applies to the theory.

The widely discussed problem of applicability of PQCD in the resonance region can be easily solved empirically. Presently it is the only way to establish the boundary between the hadronic matter and the partonic one. But it is of a little help in the understanding physics of the hadronic structure which is closely related with topology of the nucleon and with fundamental symmetries. The ultimate goal is the development of an adequate approach for consideration of *quantum* phenomena of *non-perturbative* nature.

Acknowledgements

References

[1] K.F. Liu and C.W. Wong, Phys. Rev. D **28** (1983) 170.

[2] R. Hofstatder, Rev. Mod. Phys. **28** (1956) 214.

[3] R.G. Roberts, *The Structure of the Proton*, Cambridge University Press, Cambridge, 1990.

[4] V.A. Petrun'kin, Sov. Phys. JETP, 13 (1961) 808; Particles and Nuclei, 1981, Vol. 12 (3).

[5] G.A. Sokol, in *The Nucleon Compton Effect at Low and Medium Energies*, Proc. of the P.N. Lebedev Physics Institute, Vol. 41, pp.59-147, Edited by D.V. Skobel'tsyn, Consultants Bureau, New York, 1969.

[6] G. Sterman and P. Stoler, Annu. Rev. Nucl. Part. Sci. 47 (1997) 193.

[7] V.D. Burkert," Leptonic production of baryon resonances", Lectures presented at the Advanced Summer Study, Dronten, The Netherlands, August 1-14, 1993, CEBAF-PR-93-035, October 21, 1993.

[8] D. Drechsel and L. Tiator, J. Phys. G: Nucl. Part. Phys. **18** (1992) 449.

[9] D. Drechsel et al., Nucl. Phys. A **645** (1999) 145.

[10] I.G. Aznauryan and S.G. Stepanyan, Phys. Rev. D **59** (1999) 054009.

[11] A. L'vov et al., Phys. Rev. C **55** (1997) 359.

[12] N. Isgur, G. Karl and R. Koniuk, Phys. Rev. D **25** (1982) 2396.

[13] S.S. Gershtein and D.V. Dzhikiya, Sov. J. Nucl. Phys. **34** (1981) 870.

[14] M. Bourdeau and N.C. Mukhopdhyay, Phys. Rev. Lett. **58** (1987) 97; **63** (1989) 335.

[15] S. Capstick and G. Karl, Phys. Rev. D **41** (1990) 2767.

[16] F. Ravndal, Phys. Rev. D **4** (1971) 1446.

[17] R.M. Davidson, N.C. Mukhopdhyay and R. Wittman, Phys. Rev. Lett. **56** (1986) 804; Phys. Rev. D **43** (1991) 71.

[18] J. Bienkowskä, Z. Dziembowski and H.J. Weber, Phys. Rev. Lett. **59** (1987) 624.

[19] G. Kälbermann and J.M. Eisenberg, Phys. Rev. D **28** (1983) 71.

[20] G.S. Adkins, C.R. Nappi and E. Witten, Nucl. Phys. **B228** (1983) 552.

[21] A. Wirzba and W. Weise, Phys. Lett. B **188**(1987) 6.

[22] G. Eckart and B. Schwesinger, Nucl. Phys. A **458** (1986) 620; B. Schwesinger, Nucl. Phys. A **537** (1992) 253.

[23] T.D. Kohen and W. Broniowski, Phys. Rev. D **34** (1986) 3472.

[24] M. Benmerrouche and N.C. Mukhopdhyay, Phys. Rev. D **46** (1992) 101.

[25] V.F. Grushin et al., Sov. J. Nucl. Phys. **38** (1983) 881; V.F. Grushin, in *Photoproduction of Pions on Nucleons and Nuclei*, edited by A.A. Komar (Nova Science, New York, 1989), p. 1ff.

[26] M.K. Jones et al.,(JLAB Hall-A Collaboration), nucl-ex/9910005, 1999.

[27] R.C.E. Devenish and D.H. Lyth, Nucl. Phys. B **93** (1975) 109.

[28] G. Audit et al., JLAB Proposal PR-E93050 (1993), Spokespersons P. Bertin, C. Hyde-Wright, P. Guichon.

[29] Particle Data Groupe, C. Caso et al., Eur. Phys. J. C 3, 1-794 (1998).

[30] W.J. Metcalf and R.L. Walker, Nucl. Phys. B **76** (1974) 253.

[31] M. Benmerrouche and N.C. Mukhopdhyay, Phys. Rev. Lett. **67** (1991) 1070.

[32] V.V. Frolov et al., Phys. Rev. Lett. **82** (1999) 45.

[33] V.V. Burov, A.V. Molochkov and G.I. Smirnov, Particles and Nuclei, Vol. **30(6)** (1999) 1337; English translation: Vol. **30(6)** (1999) 579.

[34] S. Capstick and B.D. Keister, Phys. Rev. D **51** (1995) 3598.

[35] R. Koniuk and N. Isgur, Phys. Rev. D **21** (1980) 1869.

[36] E.D. Bloom and F.J. Gilman, Phys. Rev. D **4** (1971) 2901.

[37] S. Capstick and B.D. Keister, Phys. Rev. D **47** (1993) 860.